

S-PROCESS ELEMENT ABUNDANCES WITH THE GAIA/GSP-SPEC CATALOGUE

G. Contursi¹, P. de Laverny¹, A. Recio-Blanco¹ and P. A. Palicio¹

Abstract. The study of *s*-process elements allows to constrain and better understand the nucleosynthesis within AGBs. These evolved stars indeed release *s*-process elements at their surface through successive Third Dredge Ups.

On another hand, Galactic Archaeology relies on the study of a large amount of stars in order to statistically characterise the different Galactic stellar populations. It is in this context that the Gaia DR3 offers a huge step forward since such chemical abundances associated with accurate astrometric data have been published for an unprecedented number of stars. Thanks to such data derived from the analysis of RVS spectra by the *GSP-Spec* module, we have explored the Galactic content in neutron-capture elements (Ce, Nd) and the importance of those elements in the stellar evolution.

GSP-Spec Ce abundances cover several stellar populations (AGB and giants) while Nd abundances are available only on AGB stars. Therefore, combining Ce and Nd abundances, we found a good correlation between those two elements in AGB stars. We also found a relation between *s*-process abundances and atmospheric parameters of the stars showing the production of Ce and Nd by the AGB. We compared our *GSP-Spec* abundances with AGB models.

In addition, Gaia DR3 cerium abundances can be used to trace the Galactic content of the Milky Way. For instance, we found a flat trend in [Ce/Fe] vs [M/H] in the Milky way disc. We also computed horizontal gradient from field stars as well as from open clusters. We also found cerium in the halo within accreted systems and one globular cluster.

Keywords: Galaxy: abundances, disc, halo, evolution - Stars: abundances, evolution, AGB and post-AGB

1 Introduction

Our understanding of the Milky Way has made a great leap forward thanks to the different data releases of the Gaia mission. The third release (Gaia Collaboration et al. 2023) consists in a major and unique step since it includes a large variety of new data products including, in particular, extensive characterisation of the *Gaia* sources. In this context, the General Stellar Parametrizer from Spectroscopy module (*GSP-Spec*, hereafter, see Gaia Collaboration, Recio-Blanco et al. 2022) has estimated atmospheric parameters (effective temperature T_{eff} , surface gravity $\log(g)$, global metallicity [M/H], abundances of α -elements with respect to iron [α/Fe]) as well as individual chemical abundances of up to a dozen of elements* for about 5.6 millions stars which have been observed by the Radial Velocity Spectrometer (RVS hereafter, Katz et al. 2022). The *GSP-Spec* module also provides quality flags (*flags_gspspec* hereafter) related to the parametrization or the determination of the individual abundances.

Among these 13 chemical elements, three are produced by neutron captures in the inner layers of some specific stages of stellar evolution: Zirconium ($Z = 40$), Cerium ($Z = 58$) and Neodymium ($Z = 60$). According to the seminal work of Burbidge et al. (1957), neutron capture occurs through two main processes: the rapid (*r*-) and slow (*s*-) processes (slow and rapid referring to the time-scale of the neutron captures with respect to the β -decay).

The formation sites of the *s*-process are well understood. When looking at the distribution of Solar abundances, three peaks located around the atomic mass number $A=90$, 138 and 208 are found. Sr, Y and Zr

¹ Universit  C te d'Azur, Observatoire de la C te d'Azur, CNRS, Laboratoire Lagrange, Bd de l'Observatoire, CS 34229, 06304 Nice cedex 4, France

*see https://www.cosmos.esa.int/web/gaia/iow_20210709. These elements are: N, Mg, Si, S, Ca, Ti, Fe I, Fe II, Ni, Zr, Ce, and Nd.

represent the first peak; Ba and Ce the second and Pb the third ones. Even though all these elements are mainly formed via s-process (Prantzos et al. 2018), their formation sites can differ. Indeed, the s-process can be decomposed in three sub-processes, each one populating a different peak (see Kappeler et al. 1989, and references therein). Low- and intermediate-mass AGB stars at Solar metallicity produce the so-called *main* s-process such as Ce and Nd thanks to neutrons produced mainly by the $^{13}\text{C}(\alpha, n)^{16}\text{O}$ reaction (Bisterzo et al. 2015, e.g.). This reaction takes place in the so-called ^{13}C -pocket, between the H and He burning shells. This ^{13}C pocket is formed through a sequence reaction $^{12}\text{C}(\text{p}, \gamma)^{13}\text{N}(\beta^+)^{13}\text{C}$ thanks to the partial mixing of protons from the convective H-rich envelope into the ^{12}C region during the third dredge-up. The $^{22}\text{Ne}(\alpha, n)^{25}\text{Mg}$ reaction also contributes to the convective thermal pulse.

This work is composed as follows. Section 2 describes the study of the *GSP-Spec* Ce abundances in the Milky Way while Sect. 3 presents Ce and Nd *GSP-Spec* abundances focusing on AGB. Finally, the conclusions of this work are presented in Sect. 4.

2 Cerium content of the Milky Way

In this section, we investigate the cerium content of the Milky Way, based on the *GSP-Spec* abundances. Cerium abundances are determined from a triplet of Ce II lines centred around 851.375 nm (in vacuum). An example of this cerium feature is provided in Fig. 9 of Gaia Collaboration, Recio-Blanco et al. (2022). More details about this work can be found in Contursi et al. (2023).

2.1 Sample selection

Among the about 5.6 million of stars having chemo-physical parameters derived by the *GSP-Spec* module, there are 103 948 stars with a Ce abundance, whatever the *flags_gspspec*. By selecting a specific combination of these flags, we obtained a sample of 29 941 stars with high-quality Ce abundances. This sample contains some AGB stars. As evoked in the introduction, AGB stars are among the main producers of s-process elements such as Ce. We then removed those stars from the sample as they can be polluted by internal production. s-process elements on AGB stars parametrized by *GSP-Spec* are investigated in the next section.

We then end up with a sample of 7397 stars to investigate the Ce content of the Milky Way. 90% of this sample have $|Z_{max}| < 0.7$ kpc and 85% have a total velocity < 70 km/s, confirming their belonging to the disc.

2.2 [Ce/Fe] versus [M/H] trend

We illustrate the [Ce/Fe] trend with respect to metallicity in the top panel of Fig. 1. We found a rather flat trend at a mean level of [Ce/Fe] ~ 0.2 dex for metallicities varying between ~ -0.7 up to $\sim +0.3$ dex. A similar behaviour and mean level of [Ce/Fe] is reported by Forsberg et al. (2019), based on 277 stars (red triangles in Fig. 1, top panel). This flat trend is also in agreement with Reddy et al. (2006) (178 stars), Battistini & Bensby (2016) (365 stars) and Delgado Mena et al. (2017) (orange diamonds in Fig. 1, top panel, 653 stars. Note that those stars have $T_{\text{eff}} > 5300$ K and $S/N > 100$ according to their Sect. 4), although these authors report a lower [Ce/Fe] level (around $\sim +0.0$ dex), probably resulting from different calibrations and/or reference scales. Finally, it is worth noting that, in the low metallicity regime ($[M/H] < -0.8$ dex), the working sample is probably not statistically representative.

The bottom panel of Fig. 1 shows the [Ce/Ca] abundance ratio versus [Ca/H]. Orange dots illustrate again the running mean [Ce/Ca] abundance, using bins of 0.07 dex in [Ca/H]. Error bars are the associated standard deviation for each bin. For values of [Ca/H] larger than ~ -0.7 dex (low statistics blurring the trend at lower metallicities), we found a slight increasing [Ce/Ca] abundance with increasing [Ca/H] ($\delta[\text{Ce}/\text{Ca}]/\delta[\text{Ca}/\text{H}] = 0.087^{\pm 0.013}$), similar to the trend of the high-Ia population of Griffith et al. (2021) (this population representing their thin disc low-[Mg/Fe] distribution). It is important to note that Griffith et al. (2021) used Mg abundances from APOGEE DR16 data, while the α -element reference is Ca in our study.[†] This continuous increase of [Ce/Ca] could be the consequence of the later contribution of AGB stars (main producers of s-process elements, as cerium) in the Galactic chemical evolution history with respect to SN II (producers of α -elements as Ca). Moreover, we point out that we also found a rather flat distribution of [Ce/Ca] ratio for [Ca/H] > 0.1 dex whereas Griffith et al. (2021) report a strong decrease. This is due to the different trend of our Ca abundances

[†]We adopted Ca instead of Mg as several of the *High-Quality Sample* stars do not have *GSP-Spec* magnesium abundances.

and their Mg ones. Actually, their $[\text{Mg}/\text{Fe}]$ remains constant for positive metallicities, contrary to the continuous decrease of our $[\text{Ca}/\text{Fe}]$, as it can be seen in Fig.25 of Recio-Blanco *et al.* (2022). This continuous decrease is more in agreement with Galactic evolution models that predict a similar decrease of any $[\alpha/\text{Fe}]$ ratios with $[\text{M}/\text{H}]$ (see also Spitoni *et al.* (2022)). We also note that our $[\text{Ce}/\text{Ca}]$ is systematically higher than that of Griffith *et al.* (2021), probably because of the different reference scales adopted.

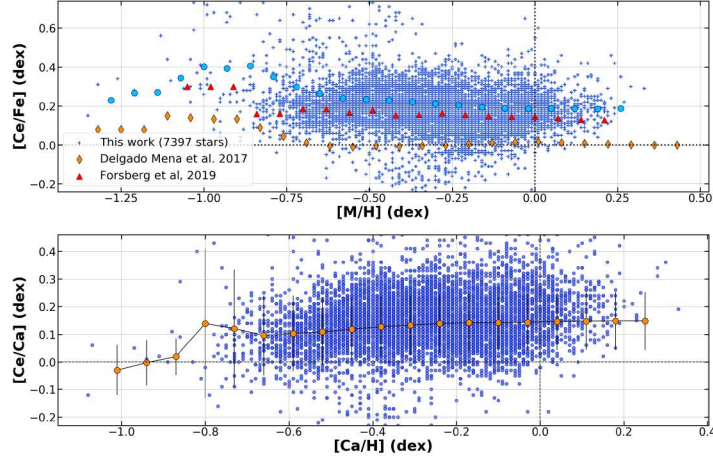


Fig. 1. Top panel: Cerium and iron abundances ratio for the *High-Quality Sample* with respect to the metallicity. Red triangles and orange diamonds are mean $[\text{Ce}/\text{Fe}]$ ratios for the stars of F19 and Delgado Mena *et al.* (2017), respectively (computed per bins of 0.07 dex). Sky blue points the mean of our data per bin of 0.07 dex in $[\text{Ca}/\text{H}]$. **Bottom panel:** $[\text{Ce}/\text{Ca}]$ versus $[\text{M}/\text{H}]$. Orange dots correspond to the mean of the measurements per bin of 0.07 dex and the error bars correspond to the standard deviation in each bin.

3 Production of Ce and Nd in AGB stars

We define a working sample of 19 544 AGB stars having high-quality Ce and/or Nd abundances (17 765 stars with Ce abundances and 3 490 with Nd abundances, 1 711 stars having both Ce and Nd abundances), selected by applying a specific combination of the *GSP-Spec* quality flags.

We first confirmed that the majority of the working sample is composed of AGB stars by estimating their absolute magnitude in the K-band and their properties in a Gaia-2MASS diagram. We also checked that these stars are oxygen-rich AGBs, as assumed during the *GSP-Spec* parameterisation.

Fig. 2 shows a high positive correlation between the Ce and Nd abundances (Pearson correlation coefficient = 0.75). The associated dispersion is rather large since it is dominated by the Nd measurement uncertainties, the Nd II line being more difficult to analyse. Such a correlation confirms the quality of the derived abundances since it is actually expected as both elements belong to the *s*-process second peak and hence have a similar nucleosynthetic origin. We also remark that colour-coding this correlation with T_{eff} clearly shows the enhancement of the Ce and Nd abundances for cooler stars, i.e. for more evolved stars on the AGB. This illustrates the successive mixing episodes enriching the AGB surface in *s*-process elements formed deeper in their stellar interior.

We then compared the observed Ce and Nd abundances with FRUITY and Monash AGB yields and found that the higher Ce and Nd abundances can not be explained by AGBs of mass higher than $5 M_{\odot}$. On the contrary, the yields predicted by both models for AGB with an initial mass between ~ 1.5 and $\sim 2.5 M_{\odot}$ and metallicities between ~ -0.5 and ~ 0.0 dex are fully compatible with the observed *GSP-Spec* abundances.

Note that more details about this work can be found in Contursi *et al.*, in prep.

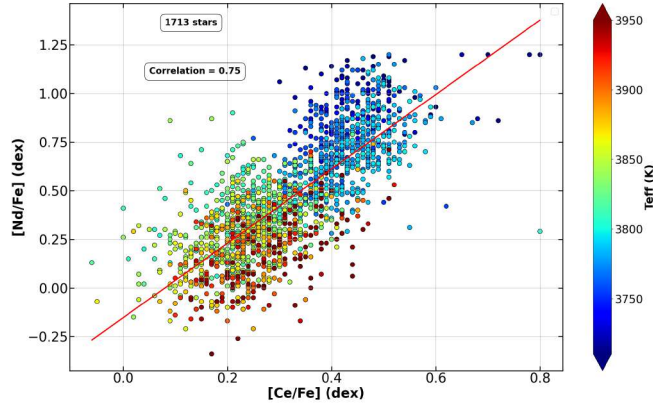


Fig. 2. Correlation between Ce and Nd abundances for AGB stars colour-coded by their T_{eff} . The slope of the red line is 1.91 while the standard deviation is 0.44 dex. The Pearson correlation coefficient is also reported.

4 Conclusions

The Gaia DR3 is the first whole-sky spatial spectroscopic survey. Among the 5.6 million of stars parametrized by the *GSP-Spec* module, some of them have abundances of elements formed through neutron capture: cerium and neodymium.

We first investigate the cerium content of the Milky Way and found a relatively flat trend with the metallicity. We compared it with literature measurements.

On the other hand, we investigated the Ce and Nd abundances in AGB stars parametrized by *GSP-Spec* and found higher abundances of these elements for cooler stars (i.e. in more advanced stages for a given $\log(g)$ and $[M/H]$).

All those results show the excellent quality of the Gaia DR3 data and are in agreement with our understanding of the production sites of these elements as well as their evolution through the Galactic chemical evolution history.

References

- Battistini, C. & Bensby, T. 2016, *A&A*, 586, A49
 Bisterzo, S., Gallino, R., Käppeler, F., et al. 2015, *MNRAS*, 449, 506
 Burbidge, E. M., Burbidge, G. R., Fowler, W. A., & Hoyle, F. 1957, *Reviews of Modern Physics*, 29, 547
 Contursi, G., de Laverny, P., Recio-Blanco, A., et al. 2023, *A&A*, 670, A106
 Delgado Mena, E., Tsantaki, M., Adibekyan, V. Z., et al. 2017, *A&A*, 606, A94
 Forsberg, R., Jönsson, H., Ryde, N., & Matteucci, F. 2019, *A&A*, 631, A113
 Gaia Collaboration, Vallenari, A., Brown, A. G. A., et al. 2023, *A&A*, 674, A1
 Gaia Collaboration, Recio-Blanco, A., Kordopatis, G., de Laverny, P., et al. 2022, arXiv e-prints, arXiv:2206.05534
 Griffith, E., Weinberg, D. H., Johnson, J. A., et al. 2021, *ApJ*, 909, 77
 Käppeler, F., Beer, H., & Wisshak, K. 1989, *Reports on Progress in Physics*, 52, 945
 Katz, D., Sartoretti, P., Guerrier, A., et al. 2022, arXiv e-prints, arXiv:2206.05902
 Prantzos, N., Abia, C., Limongi, M., Chieffi, A., & Cristallo, S. 2018, *MNRAS*, 476, 3432
 Recio-Blanco, A., de Laverny, P., Palicio, P. A., et al. 2022, arXiv e-prints, arXiv:2206.05541
 Reddy, B. E., Lambert, D. L., & Allende Prieto, C. 2006, *MNRAS*, 367, 1329
 Spitoni, E., Recio-Blanco, A., de Laverny, P., et al. 2022, arXiv e-prints, arXiv:2206.12436